Modeling of slow strain rate corrosion testing of austenitic stainless steel through continuum damage mechanics

Ivan Napoleão Bastos
Instituto Politécnico, Universidade do Estado do Rio de Janeiro, Nova Friburgo, RJ – Brazil

José Antonio da Cunha Ponciano Gomes
PEMM/COPPE / Universidade Federal do Rio de Janeiro, Rio de Janeiro, RJ – Brazil

Heraldo Silva da Costa Mattos
Laboratório de Mecânica Teórica e Aplicada, Departamento de Engenharia Mecânica, Universidade Federal Fluminense, Niterói, RJ – Brazil

Abstract

Slow strain rate testing is widely used on stress corrosion cracking research as the basic experimental technique to promote the incidence of cracking and to determine the ranking of susceptibility of different alloys in several corrosive environments. With this methodology, however, the assessment of "threshold values" to be used as design parameters is not a simple task in the present state of art of the corrosion area. This limitation induces the use of the SSR testing as "go-no go" test for materials selection and some basic information required, for instance, time to failure in service, can not be inferred by this approach. The most important reason for the limitation described is the complexity of stress corrosion mechanism that involves the conjoint action of mechanical and electrochemical processes. On the present work, a methodology for modeling SSR testing based upon thermodynamics of continuum solids and elasto-plastic damage is proposed. In this macroscopic approach, besides the classical variables (stress, total strain, plastic strain), an additional scalar variable related with the damage induced by stress corrosion is introduced. An evolution law with environment dependent parameters is proposed for this damage variable. The model accounts for the stress corrosion effect through a reduction of the mechanical resistance of the material induced by the damage variable. The model prediction is compared with the curves obtained experimentally in different acid solutions at room temperature showing a good agreement. The alloy/environments system is 304 austenitic stainless steel/acid chloride solutions.

Keywords: slow strain rate test, constant load test, damage mechanics, stress corrosion cracking, stainless steel

Mechanics of Solids in Brazil 2007, Marcílio Alves & H.S. da Costa Mattos (Editors)
Brazilian Society of Mechanical Sciences and Engineering, ISBN 978-85-85769-30-7

Nomenclature

SSR	slow strain rate test
CL	constant load test
D	damage (related to the loss of mechanical strength), dimensionless
L_0	gauge length, mm
A_0	cross-section, mm^2
σ	stress, MPa
σ_p	yield stress, MPa
Y	elastic limit, MPa
ε	deformation, dimensionless
ε_p	plastic deformation, dimensionless
E	Young modulus, GPa
K	material constant, MPa.s
N	material constant, dimensionless
v_1	material constant, MPa
v_2	material constant, dimensionless
η	material constant, $MPa.h^{-1}$
S	parameter dependent on the material and environmental conditions, MPa.s
R	parameter dependent on the material and environmental conditions, dimensionless
T	time, s or h
a	damage coeficient, dimensionless

Subscripts

P	relative to plasticity
e	relative to elasticity
r	relative to rupture
CR	relative to critical value
$_0$	relative to initial conditions

1 Introduction

Stress corrosion cracking (SCC) remains as one of the most severe limitations for the use of austenitic stainless steels on chemical and petrochemical industries. The combined effect of corrosion and mechanical stress imposed on the material is extremely complex. The mechanisms proposed to explain microscopically the cracking initiation and propagation processes are not able to elucidate all aspects of

Mechanics of Solids in Brazil 2007, Marcílio Alves & H.S. da Costa Mattos (Editors)
Brazilian Society of Mechanical Sciences and Engineering, ISBN 978-85-85769-30-7

this phenomenon in different metal/environment systems [1]. Therefore attempts to predict this phenomenon in macroscopic scale models are advisable.

Slow strain rate and constant load tests are widely used on stress corrosion cracking research as the basic experimental technique to promote the incidence of cracking and to determine the ranking of susceptibility of different alloys in several corrosive environments. With this methodology, however, the assessment of "threshold values" to be used as design parameters is not a simple task in the present state of the art of material research. This limitation induces the use of the SSR and CL testing only as "go-no go" test for material selection. Some basic information required, for instance, time to failure in service, that can not be inferred from this procedure. The most important reason for the limitation described is the complexity of stress corrosion mechanism that involves the conjoint action of mechanical and electrochemical processes.

Despite the lack of definition of a fundamental mechanism for stress corrosion cracking, the evaluation of the susceptibility to cracking is a basic requirement for safe and economic operation of many types of equipments. This objective is accomplished by the execution of a set of laboratory tests that simulates the conditions of SCC incidence. In this situation, slow strain rate testing is the most important technique used to rank the susceptibility of different materials in a specific environment. Constant load and constant displacement tests are frequently used as auxiliary techniques in order to obtain more detailed information about the resistance of the material. These tests, however, do not provide basic parameters to be directly used in engineering design or to determine the "safe life" of equipment. This limitation can be explained as a consequence of the nonexistence of a model to interpret the macroscopic behavior of the material registered during the SCC tests.

The most interesting possibilities of macroscopic modeling of stress corrosion testing are provided by fracture mechanics and continuum damage mechanics. In the case of continuum damage mechanics, the damage is taken into account through an internal variable related to the loss of mechanical strength of the system due to the damage (geometrical discontinuities induced by the deformation process). Besides, this approach introduces the possibility of considering important physical phenomena like hardening, plasticity, viscoplasticity and corrosion.

2 Experimental procedures

Slow strain rate (SSR) and constant load (CL) tests were performed at different acid environments with chloride ions. In these tests it was used an AISI 304 stainless steel with the chemical composition given in Table 1.

Table 1: Composition of AISI 304 austenitic stainless steel (wt%).

Element	C	S	Ni	Si	Mo	Mn	Cr	Fe
Wt %	0.06	0.005	8.03	0.47	0.03	1.40	18.95	Bal.

Mechanics of Solids in Brazil 2007, Marcílio Alves & H.S. da Costa Mattos (Editors)
Brazilian Society of Mechanical Sciences and Engineering, ISBN 978-85-85769-30-7

The steel was previously normalized at 1050 ° C for 30 minutes in argon atmosphere furnace and water-quenched. The surface of the samples was ground to grit 600 with emery paper. After surface preparation, the samples were washed with distilled water and alcohol, and dried with hot air. The round specimens were designed according to ASTM E-8 standard with 4 mm nominal diameter and 16 mm gauge length. The samples were loaded with 1.5 yield stress in the constant load testing and the strain rate used on slow strain rate testing was 3×10^{-6}s $^{-1}$. The aerated solutions were prepared from 1 M sodium chloride acidified with 1 M chloride acid to adjust the desired pH. All the measurements were performed at room temperature under free corrosion potential.

3 Theoretical modeling

In this paper, a theoretical analysis, developed within the framework of continuum damage mechanics by [2], is performed to provide a better understanding of the results from slow strain rate test and constant load test. All the proposed equations can be developed from thermodynamic arguments that are not presented here for sake of brevity. A more detailed discussion may be found elsewhere [3, 4].

Consider as a system a bar-type tension specimen with gauge length L_o and cross-section A_0 submitted to a prescribed displacement. The basic idea is to introduce a macroscopic variable $D \in [0, 1]$, related to the loss of mechanical strength of the system due to the damage (geometrical discontinuities induced by mechanical deformation and the simultaneous corrosion processes). If $D = 0$, the bar is considered "virgin" and if $D = 1$, it is "broken" (it can no longer resist to mechanical loading). The following model is proposed to describe the coupling between elastoplasticity and the damage induced by the stress corrosion phenomenon:

$$\sigma = (1 - D)\, E\, (\varepsilon - \varepsilon_p) \tag{1}$$

$$Y = (1 - D)\left[v_1\left(1 - e^{-v_2 \varepsilon_p}\right) + \sigma_p\right] \tag{2}$$

$$\frac{d\varepsilon_p}{dt} = \left\langle \frac{\sigma - Y}{K} \right\rangle^N \tag{3}$$

$$\frac{dD}{dt} = \frac{\eta \sigma^2}{E\,(1 - D)^a}\,(\dot{\varepsilon})^P + \left(\frac{S\sigma}{(1 - D)}\right)^R \tag{4}$$

where $\langle x \rangle = \max(0, x)$ and the variables σ, ε, ε_{p} are defined as follows

$$\sigma = \frac{F}{A}; \varepsilon = \frac{\Delta L}{L_o}; \varepsilon_P = \frac{\Delta L_P}{L_o}; \Delta L = \Delta L_E + \Delta L_P \tag{5}$$

with $\Delta \mathrm{L}_e$ being the elastic or reversible part of ΔL and $\Delta \mathrm{L}_p$ the plastic or irreversible parcel of ΔL. These variables coincide, respectively, with the nominal axial stress, the axial strain and the axial plastic strain while the system is submitted to a uniaxial stress state. In the presence of macro cracks the actual state of stress is no longer uniaxial and the variables σ, ε, ε_p must be interpreted as global parameters. Y is an auxiliary variable related to the hardening induced by plastic deformation. E,

Mechanics of Solids in Brazil 2007, Marcílio Alves & H.S. da Costa Mattos (Editors)
Brazilian Society of Mechanical Sciences and Engineering, ISBN 978-85-85769-30-7

K, N, v_1, v_2, σ_p, η and a are material constants and S, R parameters which depend on the material and environmental conditions. Equations (1) and (2) will be called the state laws and equations (3) and (4) the evolution laws. Normally the evolution laws are used considering a "virgin" initial state: $\varepsilon_{\mathrm{p}}(t=0)=0$ and $\mathrm{D}(t=0)=0$. From equations (2) and (3) we have:

$$\frac{\mathrm{d}\varepsilon_{\mathrm{p}}}{\mathrm{dt}} = 0 \mathrm{if} \sigma \leq \mathrm{Y} \tag{6}$$

$$\sigma = (1-D)\left[v_1\left(1-e^{-v_2\varepsilon_p}\right)+\sigma_p\right] + K\left(\frac{d\varepsilon_p}{dt}\right)^{1/N}, if\sigma > Y \tag{7}$$

The variable Y is the elastic limit, which is affected by the plasticity phenomenon (that causes an increasing of the elastic limit $\Rightarrow \frac{dY}{d\varepsilon_p} \geq 0 \forall D \in [0,1], \forall \varepsilon_p \geq 0$) and by the damage (that causes a decreasing of the elastic limit $\Rightarrow \frac{dY}{dD} \leq 0 \forall D \in [0,1], \forall \varepsilon_p \geq 0$). Equation (7) with $D=0$ is a classical expression for elasto-viscoplastic materials [2]. The experimental identification of the parameters K, N, v_1, v_2 and σ_p is reasonably simple and it is described in this reference. The parcel $[v_1(1-e^{-v_2\varepsilon_p})+\sigma_p]$ models the non-linear relationship between the elastic limit Y and the plastic deformation ε_p. This expression is verified experimentally and is found in literature [2].

The term $K(d\varepsilon_p/dt)^{1/N}$ in equation (7) is related to the viscosity-hardening and is responsible for the dependency of the elastic limit on the rate of plastic deformation. The constant σ_p corresponds to the elastic limit when the strain rate is very small ($\dot{\varepsilon}_{\mathrm{p}} \to 0$).

The variable D is related to the reduction of the free energy of the mechanical system due to the damage induced by the deformation process and corrosion. From (2), it is simple to verify that $Y \to 0$ when $D \to 1$. It is also possible to verify from (7) that $\sigma \to 0$ when $D \to 1$. The evolution law (4) for the damage variable may be divided in two parts: one related to the plastic deformation and other related to the stress corrosion cracking.

$$\frac{dD}{dt} = \underbrace{\frac{\eta\sigma^2}{E(1-D)^a}(\dot{\varepsilon})^P}_{plasticity} + \underbrace{\left(\frac{S\sigma}{(1-D)}\right)^R}_{stresscorrosion} \tag{8}$$

where the first parcel is the plastic damage and the second corresponds to the corrosion damage. If the rate of plastic deformation is equal to zero, there is no evolution in the plastic damage

$$\underset{plast}{\dot{D}} = \frac{\eta\sigma^2}{E(1-D)^a}(\dot{\varepsilon})^P = 0 \tag{9}$$

Supposing that the plastic damage is negligible in a constant load test ($\sigma = \sigma_0 = \text{constant}$), it is possible to find the analytical solution of the differential equation that governs the damage evolution

$$\frac{dD}{dt} = \dot{D}_{corr} = \left(\frac{S\sigma_o}{(1-D)}\right)^R \quad \text{with} \quad D\,(t=0) = 0 \tag{10}$$

The solution of the equation (10) is

$$D(t) = 1 - \left[1 - \left(t\,(R+1)\,(S\sigma_o)^R\right)\right]^{\frac{1}{R+1}} \tag{11}$$

Since rupture occurs when $D = 1$, it is possible to compute the time t_r until the rupture

$$D = 1 - \left(1 - \frac{t}{t_r}\right)^{\frac{1}{(R+1)}} \quad \text{with} \quad t_r = \frac{1}{R+1}\,(S\sigma_o)^{-R} \tag{12}$$

The evolution law for the stress corrosion damage would be similar to the creep damage law proposed by [5].

From the equations here proposed it is possible to observe that during the slow strain rate tests the damage variable increases slowly until almost the end of the test ($t = t_r$) when it increases very fast until rupture ($D = 1$), as it is shown in Fig. 1.

If this kind of damage behavior is observed, it is usual to consider a critical value D_{cr} of the damage variable, beyond which the evolution to the value toward $D = 1$ is so fast that it can be considered instantaneous. If, in a conservative approach, the failure is considered to occur when $D = D_{cr}$, the following expression is obtained

$$D = 1 - \left[1 - \left(\frac{t}{t_{cr} + \frac{(1+D_{cr})^{R+1}}{R+1}\,(S\sigma_o)^{-R}}\right)\right]^{\frac{1}{R+1}} \quad \text{with} \quad \mathrm{t_{cr}} = \frac{1-(1-\mathrm{D_{cr}})^{R+1}}{R+1}\,(\mathrm{S\sigma_o})^{-\mathrm{R}} \tag{13}$$

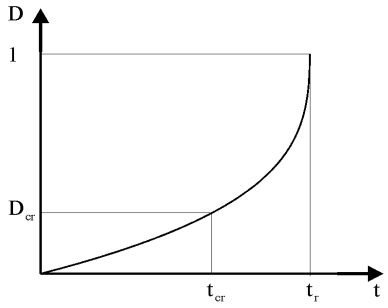

Figure 1: Schematic stress corrosion damage evolution in a slow strain rate test.

Equation (12) or (13) allows to obtain curves of the damage evolution for constant load tests under different conditions. Examples of these curves are shown in the next section. It is interesting to remark

that the parameters R and S are not independent and are related to t_{cr} through relation presented in (13). The experimental determination of the parameters R and S for a given pH is possible from an unique slow strain rate test and one constant load test and from a single constant load test the value of t_{cr} is obtained. Since σ_o and t are fixed, the parameters R and S will be related through equation (13). Hence, it is only necessary to identify the value of R in a tensile test.

To understand how the model describes the evolution of the deformation in a constant load test ($\sigma = \sigma_o = \text{constant}$), it is necessary to derive equation (1).

$$\begin{gathered}\sigma = (1-\mathrm{D})\,\mathrm{E}\,(\varepsilon - \varepsilon_{\mathrm{p}}) \Rightarrow \dot{\sigma} = (1-\mathrm{D})\,\mathrm{E}\,(\dot{\varepsilon} - \dot{\varepsilon}_{\mathrm{p}}) - \dot{D}\mathrm{E}\,(\varepsilon - \varepsilon_{\mathrm{p}}) \\ \Rightarrow \dot{\varepsilon} = \frac{\dot{\sigma}}{(1-\mathrm{D})\mathrm{E}} + \frac{\sigma\dot{\mathrm{D}}}{(1-\mathrm{D})^2\mathrm{E}} + \dot{\varepsilon}_{\mathrm{p}}\end{gathered} \tag{14}$$

Since σ is a constant and hence $\dot{\sigma} = 0$, it comes that

$$\dot{\varepsilon} = \frac{\sigma \dot{D}}{(1-D)^2 E} + \dot{\varepsilon}_p \tag{15}$$

As it is shown in the next section, the corrosion elongation curve is very well described by this model, also considering in the analysis the important parameters as steady state elongation rate, time to failure, etc.

4 Comparison with experimental results

To evaluate the adequacy of the model presented, samples of austenitic stainless steel were tested in constant load test and slow strain rate test, and the experimental results were checked with the model. The model parameters identified experimentally for this alloy are given by:

E= 193.000 [MPa]; K = 95.336 [MPa s], N = 165; a = 52; $\eta = 0.013$ [MPa h^{-1}]. Based on experimental observations, it was adopted the following critical value for the damage: D_{cr}= 0.13.

$$S[Mpa/h] = \begin{cases} 1/13000 \text{forpH} = 1.00 \\ 1/472.52 \text{forpH} = 0.00 \\ 1/1358.63 \text{forpH} = 0.50 \\ 0 \text{forair} \end{cases} \quad R = \begin{cases} 2.3 \text{forpH} = 1.00 \\ 35.0 \text{forpH} = 0.00 \\ 6.0 \text{forpH} = 0.5 \\ 0 \text{forair} \end{cases}$$

5 Constant load tests

In this section, the results of constant load (CL) tests performed in different environments are compared with the model previsions. For the CL tests, equation (1) was rewritten as $\varepsilon(t)$ then the curves were calculated using equations (2), (3), (4) and the next equation

$$\varepsilon = \frac{\sigma}{(1-D)\,E} + \varepsilon_p \tag{16}$$

The ordinary differential equations (3) and (4) were solved using embedded 4^{th} order Runge-Kutta Cash-Karp method with 5^{th} order error estimate. The variable order Runge–Kutta method is a family of explicit Runge–Kutta formulas. Each member of the family consists of a fifth-order formula that includes embedded formulas of orders from 1 to 4. A proper order formula is chosen by calculating the solution at several different orders before the full Runge–Kutta step is computed. The detailed algorithm is included in the work of [6].

Figure 2 shows the theoretical and experimental corrosion elongation curves at a constant initial stress (σ_o=375 MPa) obtained in the air, and in aerated solution prepared from 1 M NaCl acidified with 1 M HCl to adjust the desired pH to 1.00 and 0.50. The model prevision is in very good agreement with the experimental results.

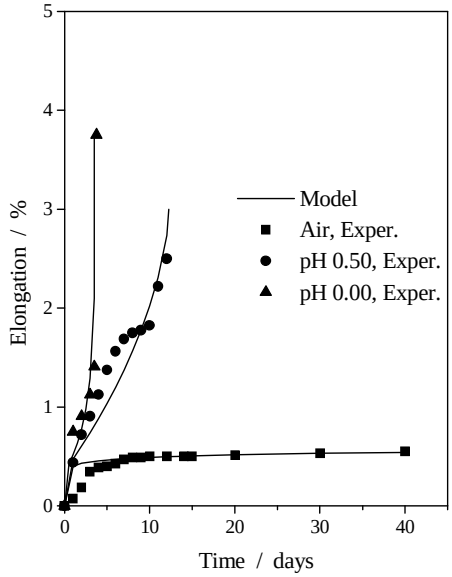

Figure 2: Elongation curves in different environments with initial σ=375 MPa.

Table 2 shows the fracture time obtained experimentally for different pHs and the theoretical value t_r obtained from solution of equation (13).

Figure 3 shows the theoretical $\sigma_0 \times \log(t_r)$ curve. The behavior is almost linear, which is in agreement with experimental observations [7] for austenitic stainless steel in acid environments at room temperature.

Table 2: Experimental and theoretical fracture time.

Condition	Experimental (h)	Model (h)
pH=0.50	372	372
pH=0.00	90.3	90.0

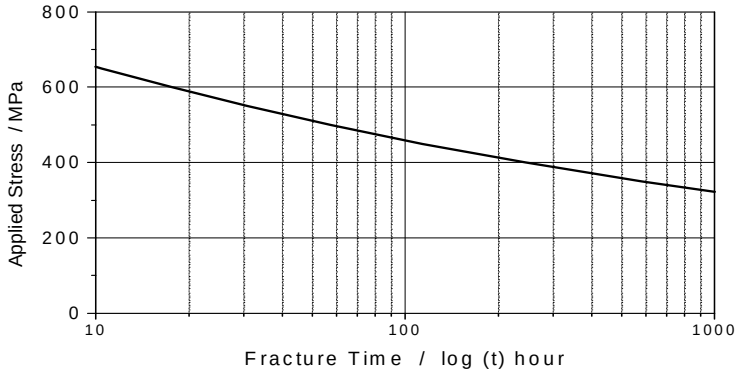

Figure 3: Model prevision of relative stress corrosion cracking resistance.

6 Slow strain rate tests

In this section, the experimental stress-strain curves obtained in slow strain rate tests performed in different environments are compared with the model previsions. Figures 4, 5 and 6 show the theoretical and experimental stress-strain curves for two different strain rates $\dot{\varepsilon} = 3 \times 10^{-6}$ s $^{-1}$ and $\dot{\varepsilon} = 2.8 \times 10^{-5}$ s $^{-1}$ obtained in the air and in aerated solution prepared from 1 M sodium chloride acidified with 1 M chloride acid to adjust the desired pH to 1.00 and 0.50. In SSR test the elongation is given by equation (17). Figures 4-6 show the stress–strain curves for $\dot{\varepsilon} = 3 \times 10^{-6}$ s $^{-1}$ and $\dot{\varepsilon} = 2.8 \times 10^{-5}$ s $^{-1}$ obtained in the air, and in aerated solutions with pH's 1.00 and 0.50. The model prevision is also in very good agreement with the experimental results.

$$\varepsilon = \dot{\varepsilon}\, t \tag{17}$$

In this case, the $\sigma\,(t)$ curves were calculated using equations (1), (2), (3) and (4). The ordinary differential equations (3) and (4) were solved using the same Runge-Kutta algorithm used in CL test simulations.

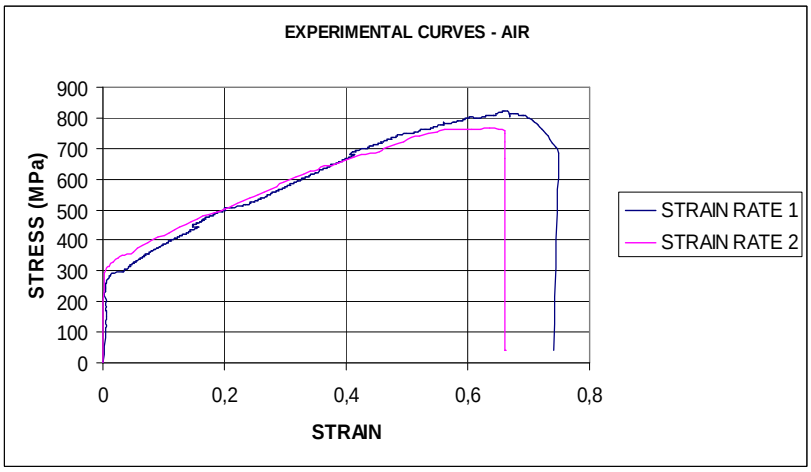

Figure 4: Stress-strain curves for $\dot{\varepsilon}_1 = 3 \times 10^{-6}$ s $^{-1}$ and $\dot{\varepsilon}_2 = 2.8 \times 10^{-5}$ s $^{-1}$ obtained in the air

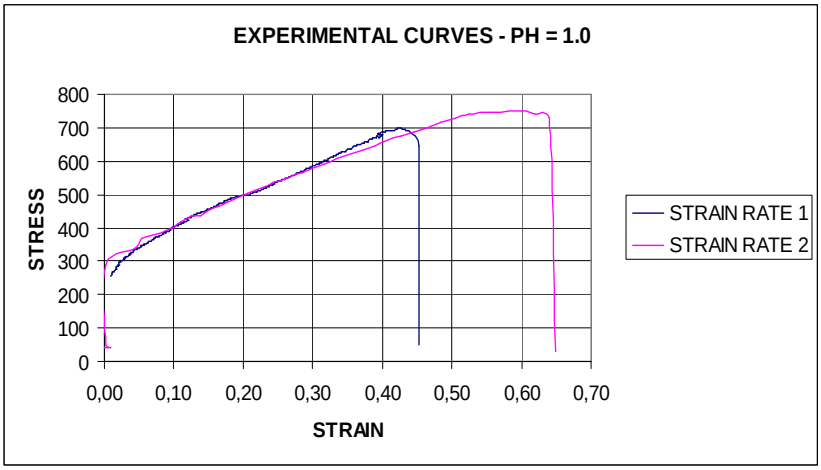

Figure 5: Stress-strain curves $\dot{\varepsilon}_1 = 3 \times 10^{-6}$ s $^{-1}$ and $\dot{\varepsilon}_2 = 2.8 \times 10^{-5}$ s $^{-1}$. pH=1.0.

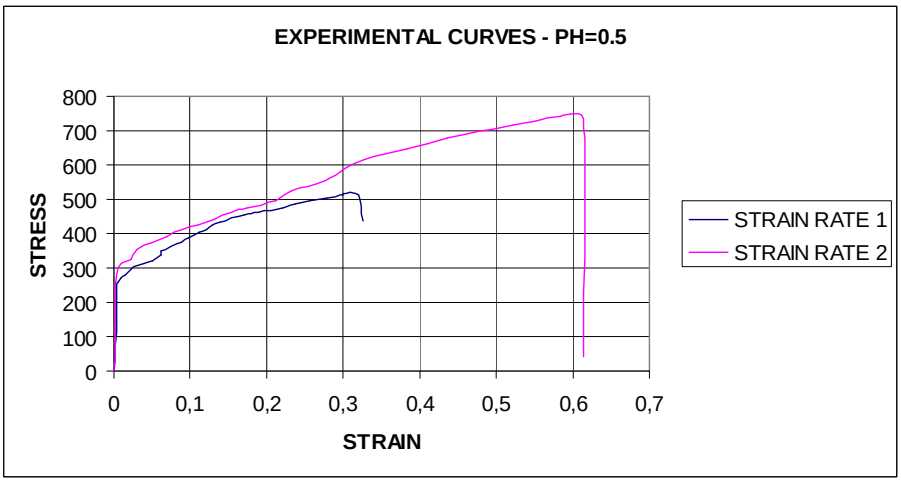

Figure 6: Stress-strain curves for $\dot{\varepsilon}_1 = 3 \times 10^{-6}$ s $^{-1}$ and $\dot{\varepsilon}_2 = 2.8 \times 10^{-5}$ s $^{-1}$. pH=0.5

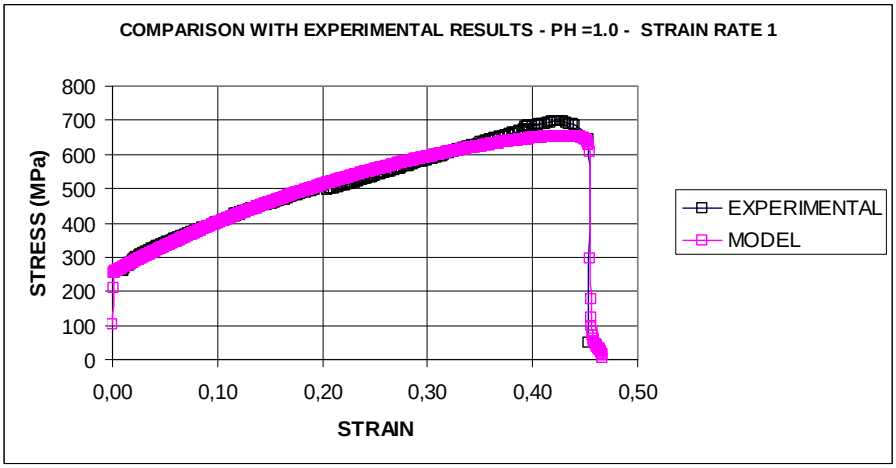

Figure 7: Comparison with experimental results. Stress–strain curves for $\dot{\varepsilon}_1 = 3 \times 10^{-6}$ s $^{-1}$. pH=1.0.

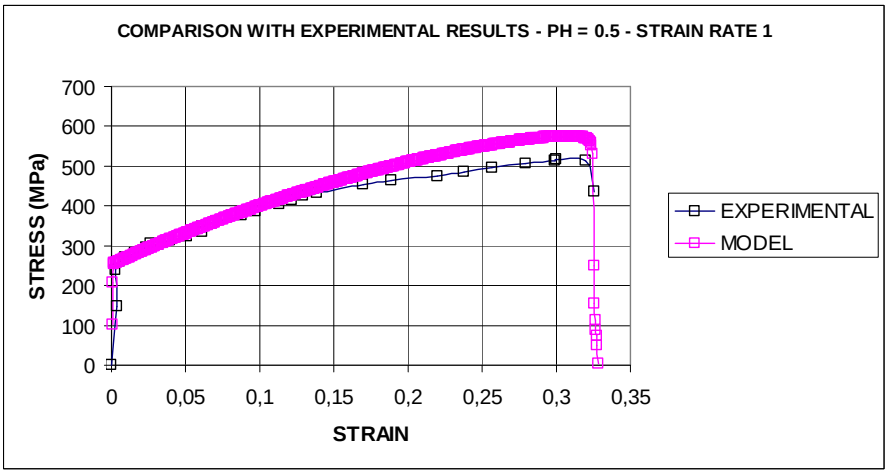

Figure 8: Comparison with experimental results. Stress–strain curves for $\dot{\varepsilon}_1 = 3 \times 10^{-6}$ s $^{-1}$. pH=0.5.

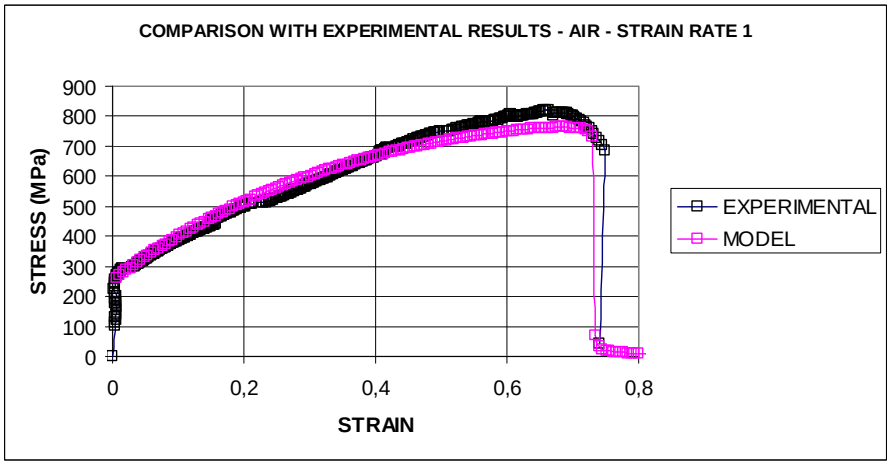

Figure 9: Comparison with experimental results. Stress–strain curves for $\dot{\varepsilon}_1 = 3 \times 10^{-6}$ s $^{-1}$. Air.

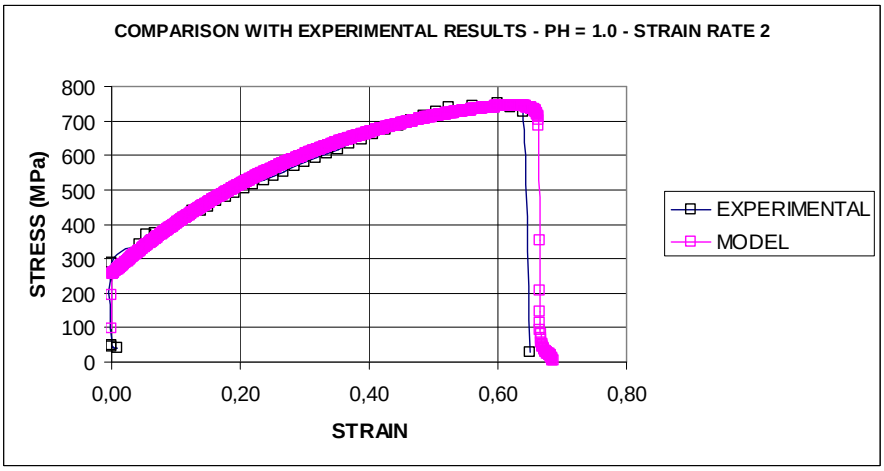

Figure 10: Comparison with experimental results. Stress–strain curves for $\dot{\varepsilon}_2 = 2.8 \times 10^{-5}$ s $^{-1}$. pH $=$ 1.0.

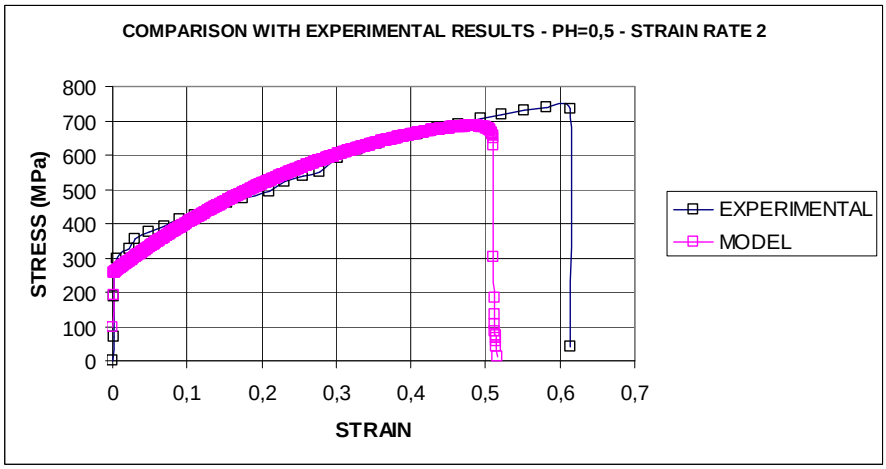

Figure 11: Comparison with experimental results. Stress–strain curves for $\dot{\varepsilon}_2 = 2.8 \times 10^{-5}$ s $^{-1}$. pH=0.5.

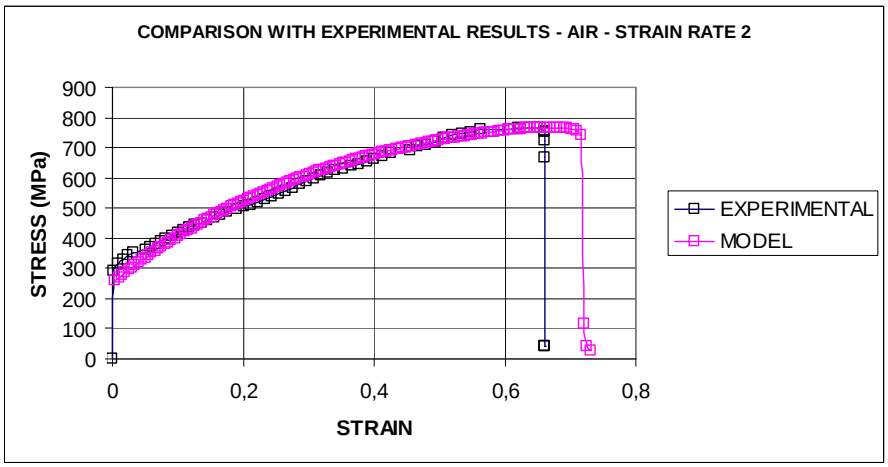

Figure 12: Comparison with experimental results. Stress–strain curves for $\dot{\varepsilon}_2 = 2.8 \times 10^{-5}$ s $^{-1}$. Air.

Figure 13 shows the damage evolution computed for the SSR tests performed at different environment with $\dot{\varepsilon}_1 = 3 \times 10^{-6}$ s $^{-1}$. From this calculation it is possible to observe that the corrosive environment strongly affects the damage evolution. This parameter shows explicitly the evolution of damage due to stress corrosion along the testing.

The damage variable presents a stable evolution until a critical experimental value $D_{cr} \approx 0.13$. After this critical value is reached, the damage increases abruptly until the limit value $D = 1$ corresponding to the fracture. At this final stage, the plastic damage is responsible for the abrupt increase of the damage rate. This behavior is in accordance with the accepted model of stress corrosion crack growth [8].

7 Conclusions

The present paper is a step towards the modeling of stress corrosion cracking phenomenon in metallic materials by using Continuum Damage Mechanics. A simple continuum damage model is proposed to describe SSR and CL tests in austenitic stainless steels. The model previsions are in good agreement with experiments where the alloy/environments system is AISI 304 austenitic stainless steel/acid chloride solutions. The results obtained by experiment and predicted parameters time of fracture and total elongation are practically identical. Thus, the agreement between theory and experiment is very good in tests performed in air or in environments with pH values equal or greater than 0.50. The effective development of corrosion damage models not only agree with experimental results as a whole, but explicit the actual damage parameters during the usual constant load and slow strain rate tests.

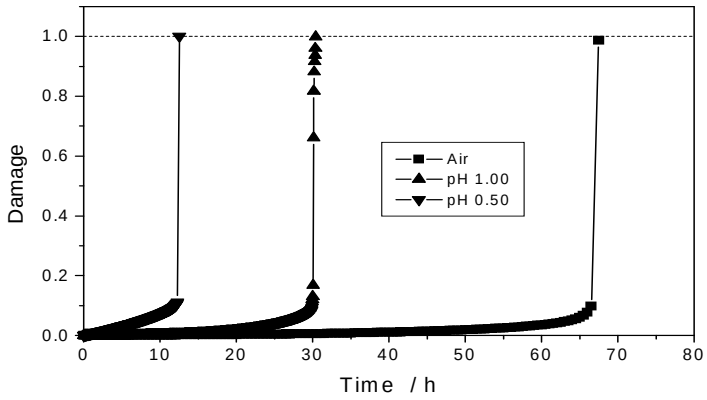

Figure 13: Damage evolution for different environments.

References

[1] Newman, R., *Stress-Corrosion Mechanisms - Corrosion Mechanisms in Theory and Practice*. Marcel Dekker Inc: New York, 1995.
[2] Lemaitre, J. & Chaboche, J., *Mechanics of Solid Materials*. Cambridge University Press, 1990.
[3] Bastos, I., *D.Sc. Thesis*. PEMM/COPPE/UFRJ: Rio de Janeiro, Brazil, 1999. (in Portuguese).
[4] Jr., J.V., *M.Sc. Dissertation*. PGMEC/UFF: Niterói, Brazil, 2002. (in Portuguese).
[5] Kachanov, M., *Introduction to Damage Mechanics*. Kluwer Academic Publishers, 1986.
[6] Cash, J. & Karp, H., A variable order runge-kutta method for initial value problems with rapidly varying right-hand sides. *ACM Trans Math Software*, **16(201-222)**, 1990.
[7] Nishimura, R. & Maeda, Y. *Corrosion Science*, **45**, p. 465, 2003.
[8] Corrosion. ASM Handbook, USA, 1996.